The Effect of Structure Modification of Sodium Compounds on the SO_2 and HCl Removal Efficiency from Fumes in the Conditions of Circulating Fluidised Bed

A. Pajdak,[a,*] B. Walawska,[b] and A. Szymanek[c]

[a]The Strata Mechanics Research Institute of the Polish Academy of Sciences, Reymonta 27, 30-059 Krakow, Poland

[b]Inorganic Chemistry Division "IChN" in Gliwice, New Chemical Syntheses Institute, Sowińskiego 11, 44-101 Gliwice, Poland

[c]Institute of Thermal Machinery, Faculty of Mechanical Engineering and Computer Science, Czestochowa University of Technology, Dąbrowskiego 69, 42-200 Czestochowa, Poland

doi: 10.15255/CABEQ.2015.2305

Original scientific paper
Received: September 21, 2015
Accepted: July 13, 2017

The article presents the effects of mechanical and thermal modification on the surface area of sodium bicarbonate and its ability to remove SO_2 and HCl from exhaust fumes.

The mechanical modification consisted of grinding in an impact mill. The thermal modification consisted of heating in the temperature range from 373 K to 673 K. The applied modifications caused a change in the grain structure of sodium bicarbonate and parameters such as specific surface area and the pore size. The parameters were determined by low-pressure nitrogen adsorption (LPNA) and mercury porosimetry (MIP) methods. The largest development of the active surface, which was up to 6 $m^2 g^{-1}$ (LPNA), was achieved after crushing and heating in the temperature range of 423–523 K.

The efficiency of a simultaneous purification of fumes from SO_2 i HCl on a continuous-combustion installation with a circular fluidised bed CFB was determined. The samples were fed into the installation in three different molar ratios 2Na/S (0.5; 1.0; 2.1) in a gas jet of 573 K. It was shown that the removal of SO_2 and HCl took place simultaneously and mainly on the grain surface. The average efficiency of SO_2 purification was between 17 % and 89 %, and it depended on the comminution degree and the amount of the sorbent. The efficiency of HCl removal was between 54 and 78 %.

Key words:
sodium bicarbonate, purification of fumes, removal of SO_2 and HCl

Introduction

Sodium compounds including sodium bicarbonate ($NaHCO_3$) are widely used in the purification of gases created by incineration of municipal and medical waste, biomass as well as alternative fuels in the cement industry. They are more often used in the energy industry and in small solid fuel combustion units including circulating fluidised bed boilers.

A number of factors determines the efficiency of using sodium compounds to purify exhaust fumes. Apart from reactivity, the size and the porosity of grains are crucial. To reduce their size, they are mechanically modified by grinding. Smaller particles, thanks to their increased active surface and a better contact with the pollutant, react faster and more efficiently than larger particles[1]. The increase in porosity is achieved through thermal modification. At high temperatures, $NaHCO_3$ decomposes into Na_2CO_3. Under industrial conditions, such decomposition takes place after placing a dry sorbent in a stream of hot exhaust gases. Sodium bicarbonate is a sorbent, which is especially suitable to be used in the dry method of flue gas purification in small power plants[2–6]. Removing SO_2 from gases using sodium bicarbonate is possible in the range of temperatures between 413 K and 573 K, and goes in two ways depending on the temperature[7–10]. In the temperature range 343–393 K it goes according to the direct model. The non-porous sodium bicarbonate of a low specific surface area reacts with the sulphur compounds only on the surface according to the reaction:

$$2NaHCO_3 + SO_2 \rightarrow Na_2SO_3 + 2CO_2 + H_2O \quad (1)$$

At temperatures above 393 K, the indirect model occurs and the direct model takes place only to a small extent. In the indirect model, the porous

*Corresponding author: pajdak@img-pan.krakow.pl

sodium carbonate with a developed active surface (2) is created as a result of the decomposition of sodium bicarbonate. In contact with sulphur dioxide, sodium(IV) sulpfate is created according to the reaction (3) and in contact with oxygen, sodium(VI) sulphate is created (4).

$$2NaHCO_3 \rightarrow Na_2CO_3 + CO_2(g) + H_2O(g) \quad (2)$$

$$Na_2CO_3 + SO_2 \rightarrow Na_2SO_3 + CO_2 \quad (3)$$

$$Na_2SO_3 + ½\ O_2 \rightarrow Na_2SO_4 \quad (4)$$

Sodium bicarbonate also shows high reactivity against hydrogen chloride[4,5,11–13]. Depending on the temperature, gas hydrogen chloride reacts with sodium bicarbonate in a direct (5) or indirect way after decomposition into sodium carbonate (2) according to the reaction (6):

$$NaHCO_3 + HCl \rightarrow NaCl + H_2O + CO_2 \quad (5)$$

$$2HCl + Na_2CO_3 \rightarrow 2NaCl + CO_2 + H_2O \quad (6)$$

In the energy industry, sodium compounds are used to remove acid gas pollutants, such as sulphur dioxide (SO_2) and hydrogen chloride (HCl) from the flue gases[14]. Along with carbon dioxide, sulphur dioxide is one of the most dangerous pollutants emitted into the atmosphere. The problem of CO_2 pollution and its removal is an extensively described issue[15–17].

Over 50 % of waste SO_2 comes from the power industry. The current concentration limits of SO_2 are regulated by EU directives including LCP directive[18] and IED directive[19], which allow the emission of SO_2 from the combustion of solids, such as coal, of up to 250 mg m^{-3}_n in plants of the nominal power of 100–300 MW and up to 400 mg m^{-3}_n in plants of 50–100 MW. The latest MCP directive[20] establishes the requirements concerning SO_2 emission for medium size combustion plants with the nominal heat output of up to 50 MW. In plants of 5–50 MW, the allowed concentration is up to 400 mg m^{-3}_n and in plants of 1–5 MW it is 1100 mg m^{-3}_n. According to the draft directive, plants of the capacity above 5 MW will be obliged to adjust their emission levels by January 1, 2025, and plants of up to 5 MW by January 1, 2030.

Removing hydrogen chloride from gases takes place mainly in installations of thermal conversion of solid waste where concentrations above 1000 mgHCl m^{-3} are noted. However, the permitted emission to the air considering average daily values is 10 mgHCl m^{-3} [21]. In installations of fuel combustion, purification of waste gases from HCl is not applied. It is connected with its low concentration in the fuels as well as the lack of proper legal acts regulating emission levels in those units. In its final preparation stage is Draft 1 LCP BREF concerning, among other, the issue of the levels of HCl and HF emitted during combustion. Its conclusions are to be published in 2016. It specifies the accepted hydrogen chloride emission for plants of the power heat of 100 MW_{th} at the level of 1–6 mg m^{-3}_n for new facilities and 2–10 mg m^{-3}_n for the existing plants, and for the plants of over 100 MW_{th} 1–3 mg m^{-3}_n and 1–5 mg m^{-3}_n respectively[22]. Taking into account the integrated protection of air and constant changes of EU acts regulating permissible emission levels, it should also be considered in such installations.

Currently in Europe, the largest application of sodium sorbents to remove SO_2 and HCl is connected with the process developed by SolvAir Solutions[23]. It involves reaction of ground bicarbonate particles with gas pollutants in a duct at temperatures around 413 K on a bag filter in which dust and reaction products are separated from the purified gas. This process provides high efficiency of exhaust purification with a low usage of the reagent as well as a low investment cost[24].

Methods and apparatus

The chemical composition of the materials used in the tests was determined by classical methods as well as LECO analysers of two types. To specify the content of carbon and hydrogen, the method of selective absorption in infrared was applied using TruSpec CHN (LECO, Poland). The concentration of nitrogen was determined using a thermal conductivity detector after reducing nitric oxides and mixing with helium. The concentration of sulphur was determined by the combustion method with IR detection using analyser SC-144 (LECO, Poland). The concentration of oxygen was determined from the difference.

Sodium bicarbonate was mechanically modified by grinding in an impact mill 160 UPZ (Hosokawa-Alpine, Germany) with the rotor speed of 11400 rpm and the efficiency of 60 kg h^{-1}. Before and after grinding, the material was subjected to a grain size analysis using a laser diffraction particle size analyser LS 13320 (Malwern, United Kingdom).

The grain structure was analysed using a scanning electron microscope XL 30 Esem (Philips, The Netherlands) with analyser EDS (EDAX, Japan), which provides real space imaging of the sample topography. The samples were dusted with gold, and using a BSE detector, images at magnification of 1000x to 20000x were recorded. The tests were carried out in the high vacuum mode at the voltage of 15 kV.

Structural parameters were measured applying porosimetric methods. The surface area and the total pore volume were defined. The measurements of microstructure of sodium bicarbonate were carried out using a Gemini VII Series Analyzer (Micromeritics Instrument Corporation, USA). The low-pressure nitrogen adsorption process (LPNA) was carried out at the temperature of 77 K. The multilayer adsorption theory Brunauer-Emmett-Teller (BET)[25] was used in the relative pressure range p/p_0 0.05–0.30. The analyses of macrostructure of $NaHCO_3$ used mercury porosimetry (MIP)[26]. The analysis were made with AutoPore IV 9500 (Micromeritics Instrument Corporation, USA). They involved the intrusion of mercury into the porous structures under the influence of strictly controlled pressure in the pressure range from 10^{-5} MPa to 414 MPa.

Thermal decomposition of $NaHCO_3$ was tested by thermogravimetric methods (TG) and differential scanning calorimetry (DSC) with a thermogravimetric analyser TGA/SDTA 851e (Mettler Toledo, Poland) and a differential scanning calorimeter DSC 822e (Mettler Toledo, Poland). The analysis was carried out in a jet of air of 50 cm^3 min^{-1}, and the heating rate of 10 K min^{-1}.

To determine the correlation of the characteristics of specific surface area and the activation temperature, correlation calculations were made. Pearson correlation coefficient was used for the analyses (7):

$$r(x,y)=\frac{cov(x,y)}{\sigma_x\cdot\sigma_y} \tag{7}$$

where:

$$cov(x,y)=E(x\cdot y)-\left[E(x)\cdot E(y)\right] \tag{8}$$

where: $r(x,y)$ – Pearson correlation coefficient between variables x and y, $cov(x,y)$ – covariance between variables x and y, σ – standard deviation, E – expected value.

The correlation coefficient takes values between –1 to 1 and is determined according to the formula (9) and (10). The result close to 0 indicates a lack of correlation of the tested characteristics, and the result close to boundary values (1, –1) indicates their strong correlation.

$$r_{xy}=\frac{\frac{1}{n}\Sigma x_i y_i-\bar{x}\,\bar{y}}{\sigma_x\cdot\sigma_y} \tag{9}$$

where:

$$r_{xy}=\frac{\Sigma(x_i-\bar{x})(y_i-\bar{y})}{\sqrt{\Sigma(x_i-\bar{x})^2(y_i-\bar{y})^2}} \tag{10}$$

where: r_{xy} – Pearson correlation coefficient, x_i – the results of particular measurements of the surface area, $\bar{x}$ – arithmetic mean from the measurements of the surface area, y_i – the results of particular measurements of the activation temperature, $\bar{y}$ – arithmetic mean of the activation temperatures.

Next, the coefficient of determination r^2 was calculated from the formula (11) and t value conclusive as for the significance of the correlation (12):

$$r^2=\frac{\Sigma(\hat{y}_i-\bar{y}_t)^2}{\Sigma(y_i-\bar{y}_t)^2} \tag{11}$$

$$t=\sqrt{n-2}\,\frac{r}{\sqrt{1-r^2}} \tag{12}$$

where: r^2 – coefficient of determination, t – value conclusive as for the significance of the correlation, n – the number of measurements.

t value was compared with critical value t_{kr} calculated from Student's t-distribution of the degrees of freedom $v = n - 2$ on the basis of which the significance level $\alpha = 0.05$ was assumed. The significance of the characteristics was determined by the fulfilment of the condition (13):

$$|t|>t_{kr} \tag{13}$$

To determine the efficiency of sodium compounds to remove SO_2 and HCl simultaneously from flue gases, the tests were carried out on a 0.1 MW CFB test rig. This original test rig is placed in the Institute of Advanced Energy Technologies in Czestochowa University of Technology in Poland. The basic element of the rig was the combustion chamber and a cyclone where the grain separation of the fluidized layer material took place. The scheme of the test rig is shown in Fig. 1.

The air and fuel were fed continuously. The fuel was supplied at the rate of 4.5 kg h^{-1}. The material of the fluidized bed in the combustion chamber was quartz sand of the grain size from 2.5 to 6.3 μm and the average grain diameter of 4.0 μm. The sodium sorbents were fed continuously into the jet of fumes in a few molar ratios (2Na/S) at a temperature of around 573 K in the second draft at Sorbent Dosing Port. After each measurement, the samples of the fly ash and bottom ash were taken at FA and BA, respectively.

To measure the concentration of gases, a GASMET DX-4000 analyser was used, which was installed at Flue Gas Sampling Port. Thanks to the application of the 'hot' method (maintaining the measurement duct at 453 K), it selectively measured the level of pollutants i.e., SO_2, HCl and O_2, CO, CO_2 as well as the moisture. The collected gas sample spectrum was analysed in CALCMET software using the FT-IR (Fourier Transform Infrared) spectroscopy method.

Based on the decrease in the concentration of the pollutants in the flue gases, the average efficien-

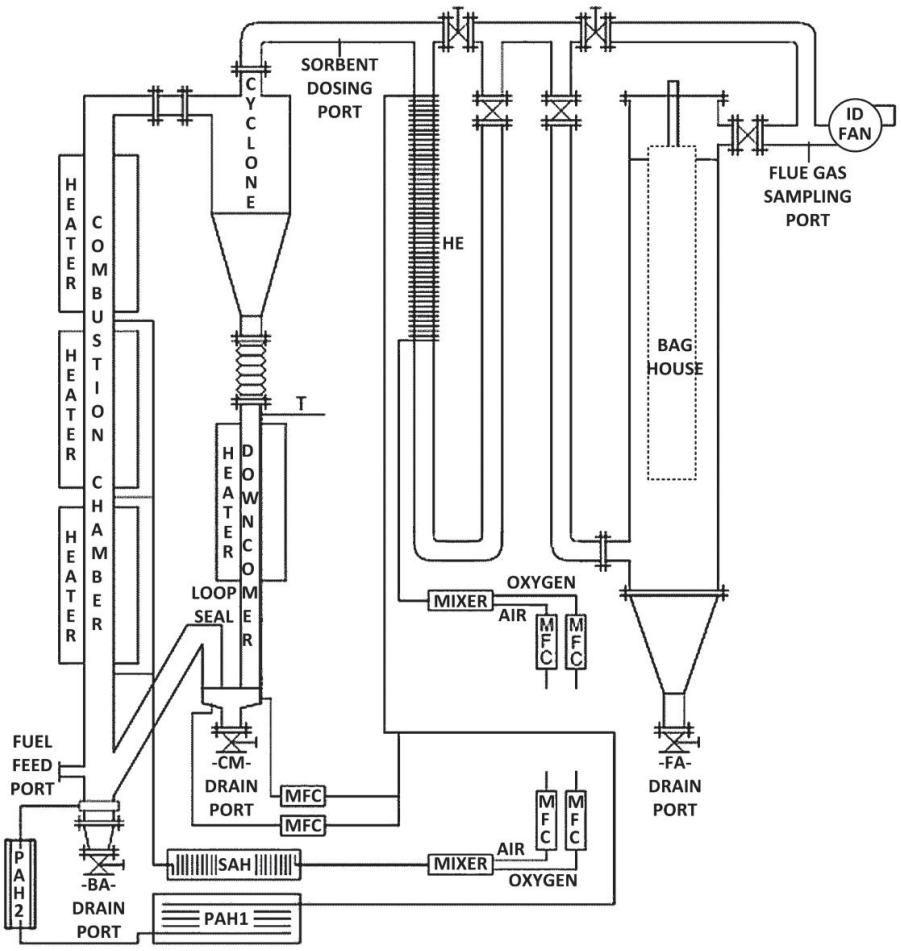

Fig. 1. – *Scheme of the CFB test rig*[27]*;*

where: BA – bottom ash, CM – circulating material, FA – fly ash, HE – heat exchanger, MFC – mass flow controller, PAH – primary air heater, SAH – secondary air heater

cy in removing SO_2 and HCl (14) as well as the maximum temporary efficiency in removing SO_2 and HCl (15) were determined according to the following formulas:

$$\varphi(t) = \frac{C_0 - C_s}{C_0} \cdot 100\ \%\ , \qquad (14)$$

where: $\varphi(t)$ – average efficiency in purifying fumes, %, C_0 – the average concentration of the pollutants in the fumes before purification (background), mg m^{-3}_n, C_s – the average concentration of the pollutants during the process, mg m^{-3}_n.

$$\varphi s(t) = \frac{C_0 - C_{min}}{C_0} \cdot 100\ \% \qquad (15)$$

where: $\varphi s(t)$ – the maximum temporary efficiency in purifying fumes, %, C_0 – the average concentration of the pollutants in the fumes before purification (background), mg m^{-3}_n, C_{min} – the minimum concentration of the pollutants during the process, mg m^{-3}_n.

Equations (14) and (15) were formulated based on the general equation for the efficiency of the process and the Clapeyron's equation. To compare the concentration levels, some simplifications were made, taking into account the conditions in which the tests were carried out, i.e. continuous flow of fumes measured in standard conditions, constant chemical composition of gases (constant concentration of pollutants (C_0), constant pressure (atmospheric), constant temperature of the gases). Due to the low concentration of pollutants, it was also assumed that the content of the remaining ingredients of gas does not change in the purification process. The concentration of SO_2 and HCl was measured continuously as the volume concentration, which was converted to mass concentration (mg m^{-3}_n), and 6 % content of oxygen.

Materials used for testing

Sodium bicarbonate ($NaHCO_3$) known as baking soda, high-purity product of standard class, comprising 99.8 % sodium bicarbonate and 0.2 % sodium carbonate (Na_2CO_3) (calculated on a dry

Table 1 – *Technical and elemental analysis of the fuel for testing*

Coal			
Technical analysis, wt.% (ad)		Elemental analysis, wt.% (ad)	
Moisture, wt.%	15.7	Carbon content (C), %	56.8
Volatile matter (V^{daf}), wt.%	32.6	Hydrogen content (H), %	3.8
Coke residue (FC^{diff}), wt.%	39.8	Oxygen content (O^{diff}), %	9.6
		Sulfur content (S), %	1.3
Ash, wt.%	11.9	Nitrogen content (N), %	0.9

Parameters determined according to the following Polish standards: V^{daf}: PN-81/G-045-04516; ash: PN-80/G-04512.
Superscript: daf-dry and ashless state; diff- calculated by difference
ad – on an air dried basis

Table 2 – *Structural characteristics of sodium bicarbonate*

Parameter	Unit	Sodium bicarbonate SO	Ground sodium bicarbonate SOm
Diameter $d_{3,2}$		45.9	4.0
Diameter $d_{4,3}$	µm	126.0	13.2
Diameter d_{50}		121.2	10.7
Mode		168.9	18.0
Coefficient of variation	%	53.4	80.5
Skewness		0.21	0.81
Surface area (LPNA)	$m^2\ g^{-1}$	0.09	0.73
Surface area (MIP)	$m^2\ g^{-1}$	0.13	1.02
Maximum pore volume (MIP)	$cm^3\ g^{-1}$	0.06	0.36

weight basis) was used as the sorbent. The material was obtained through saturation of the calcined soda produced in the Solvay process with gas CO_2 [28].

Coal from Janina coal mine in Libiąż was used as the fuel. Its characteristics are presented in Table 1.

Experimental

Sodium bicarbonate is a fine-grained material classified in accordance with the IUPAC guidelines as macroporous material[29]. It occurs in the both single grain form and as agglomerate since it has the tendency to create conglomerates. The measured mean diameter of the analysed $NaHCO_3$ was 45.9 µm ($d_{3,2}$).

As the grain size of sodium bicarbonate decreases, its reactivity increases, which is why it was ground in an impact mill. Before that it was mixed with magnesium stearate (magnesium salt of stearic acid $C_{36}H_{70}MgO_4$) – concentration 0.25 %. Adding the magnesium stearate prevented caking without affecting the physicochemical properties of $NaHCO_3$. After grinding, the obtained grains were of average diameter over ten times smaller and a larger surface area. Table 2 shows structural parameters of $NaHCO_3$ before and after grinding.

The SEM images show the grain surface before grinding (Fig. 2) and after grinding (Fig. 3). The SO grains had smooth surface and compact, crystalline structure. The SOm grains were of various sizes and irregular shapes. Furrows and cracks can be seen on their surfaces.

Grinding sodium bicarbonate, apart from developing its surface area, decreased the temperature of its decomposition. The thermogravimetric analysis showed that the maximum decomposition of the sample SO took place at 431 K (peak), whereas SOm at the temperature 414 K. Fig. 4 shows the thermogravimetric analysis of the samples.

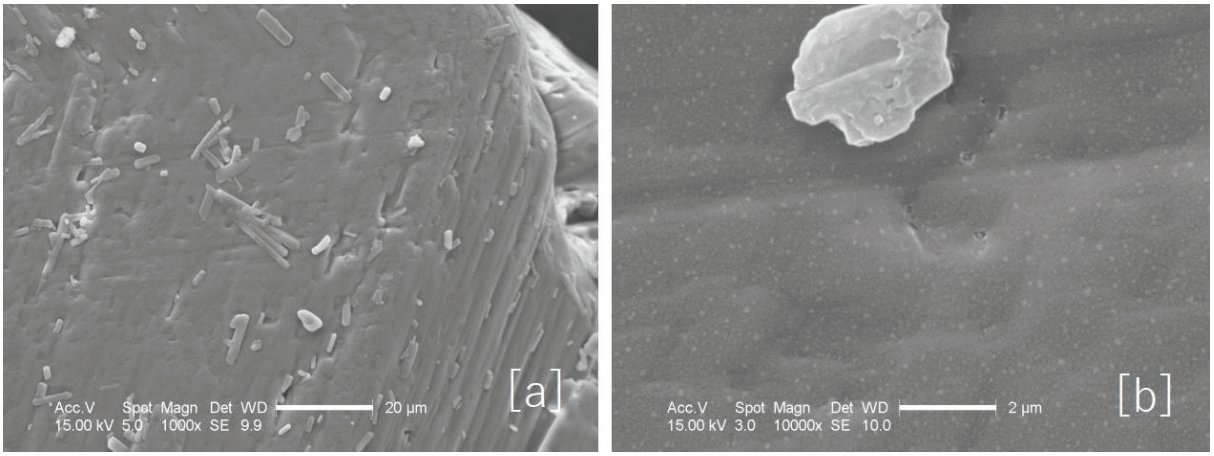

Fig. 2 – *Surface of the SO grain, BSE, magnification: a) 1000x, b) 10000x*

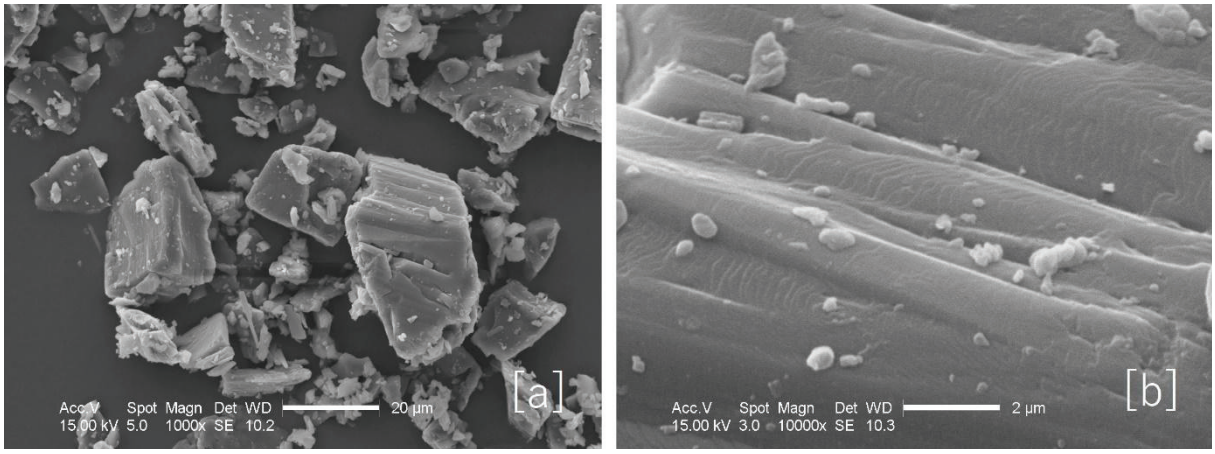

Fig. 3 – *Surface of the SOm grains, BSE, magnification: a) 1000x, b) 10000x*

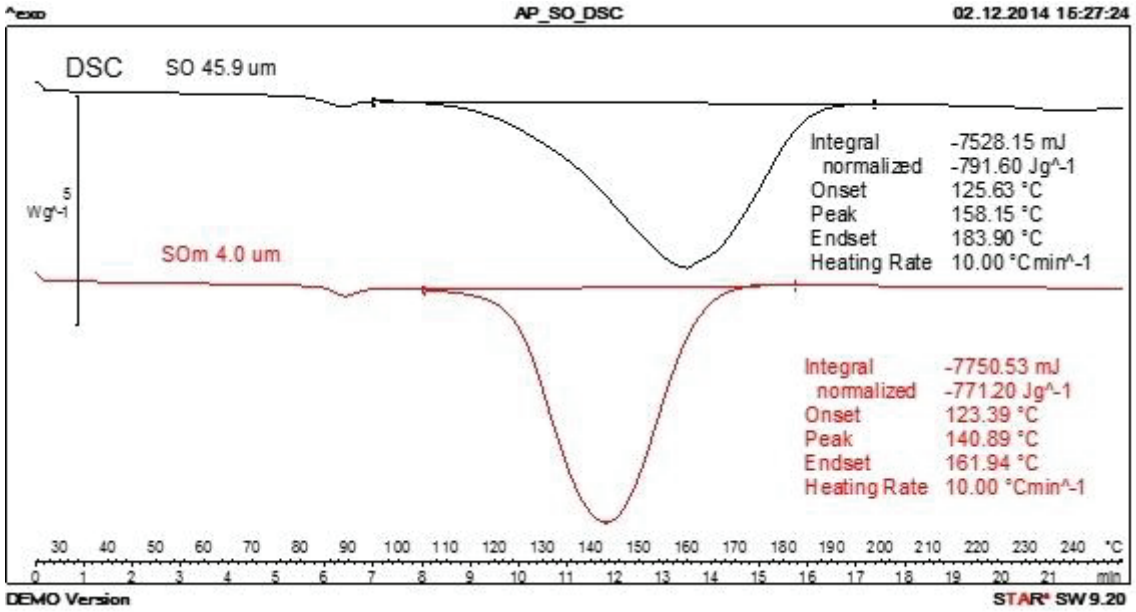

Fig. 4 – *DSC analysis of sodium compounds SO and SOm*

Before and after grinding (SO, SOm), the sodium bicarbonate was subjected to thermal decomposition by heating in the temperature range of 373–523 K for 0.5 h. After heating, LPNA and MIP methods were used to determine the following parameters: the surface area and the total pore volume. Their values changed together with the change in the activation temperature. Above the temperature of 293 K, the values of the parameters increased and in the temperature range of 423–523 K they were maximum. The surface area of the microstructure of SO sample was up to 3.2 $m^2\ g^{-1}$ (LPNA) at 473 K and SOm–6.0 $m^2\ g^{-1}$ (LPNA) at 523 K.

The maximum surface area of the sample microstructure determined by MIP method was 4.3 $m^2\ g^{-1}$ (473 K) and the maximum pore volume was 0.77 $cm^3\ g^{-1}$ (473 K). Above 523 K, the values of these parameters decreased, and at 673 K they reached the level similar to the level before the thermal modification. It was the effect of softening and closing of the pores developed in the temperature range of 293–523 K. The changes of the structural parameters are presented in Fig. 5.

The SEM analyses showed that heating the SO sample at 373 K led to the development of micrometric cracks parallel to the crystallographic directions (Fig. 6a). Small pores appeared on the surface, which resulted from partial decomposition of $NaHCO_3$ (Fig. 6b). During activation at 523 K, the SO sample decomposed totally and the pores developed more intensively than after activation at 373 K. The pores are of a more elongated shape and of a considerably bigger size, which is shown in Fig. 7.

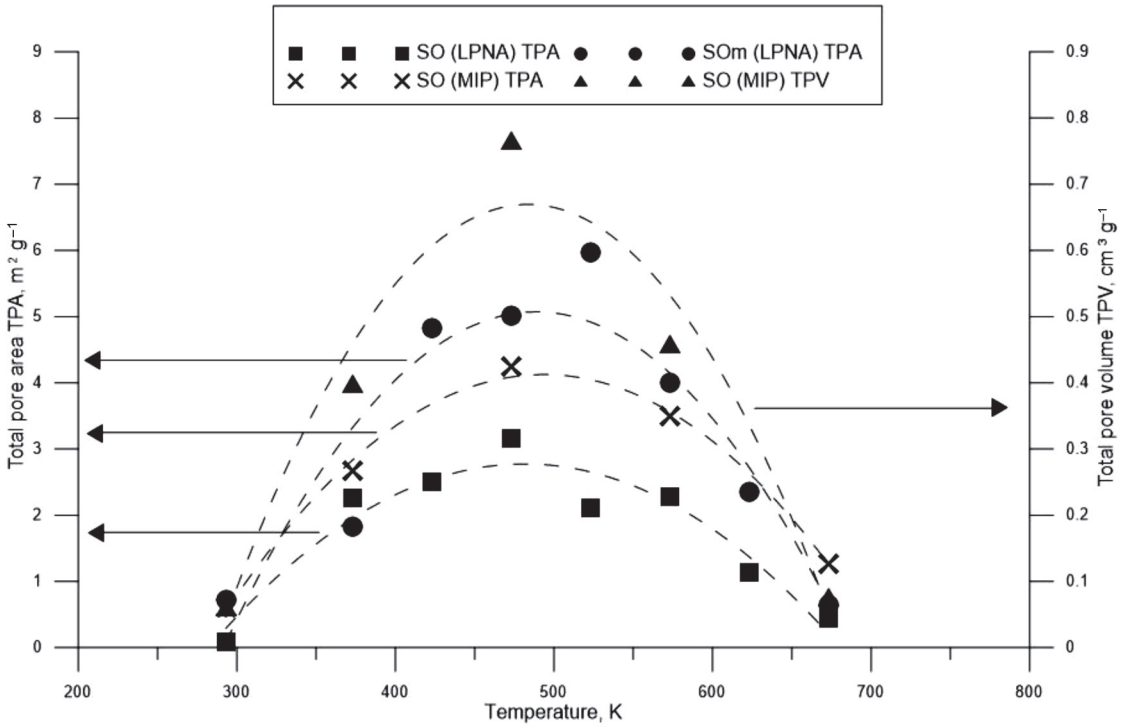

Fig. 5 – *Changes in the structural parameters of SO and SOm modified mechanically and thermally*

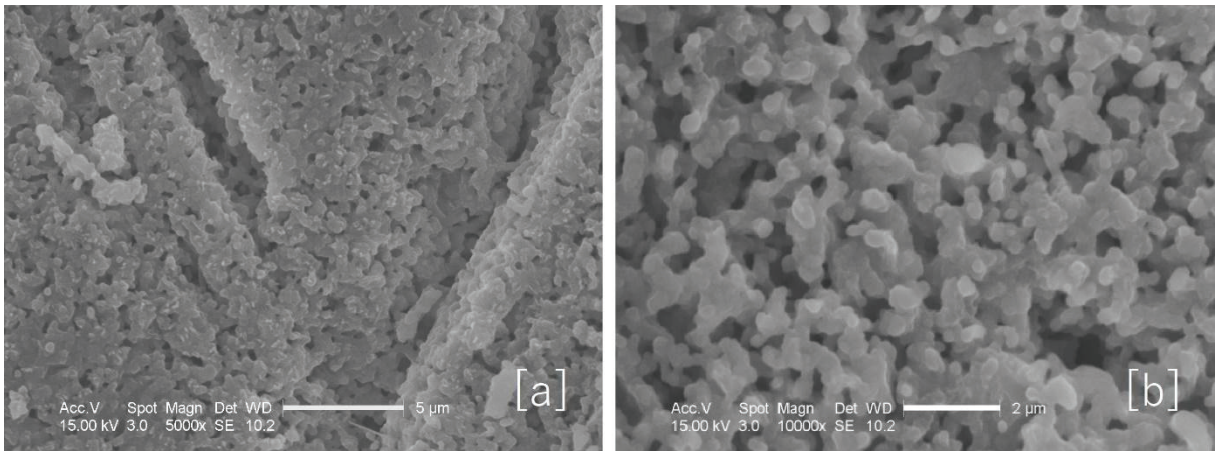

Fig. 6 – *Surface of the SO grain after thermal activation at 373 K, BSE, magnification: a) 5000x, b) 10000x*

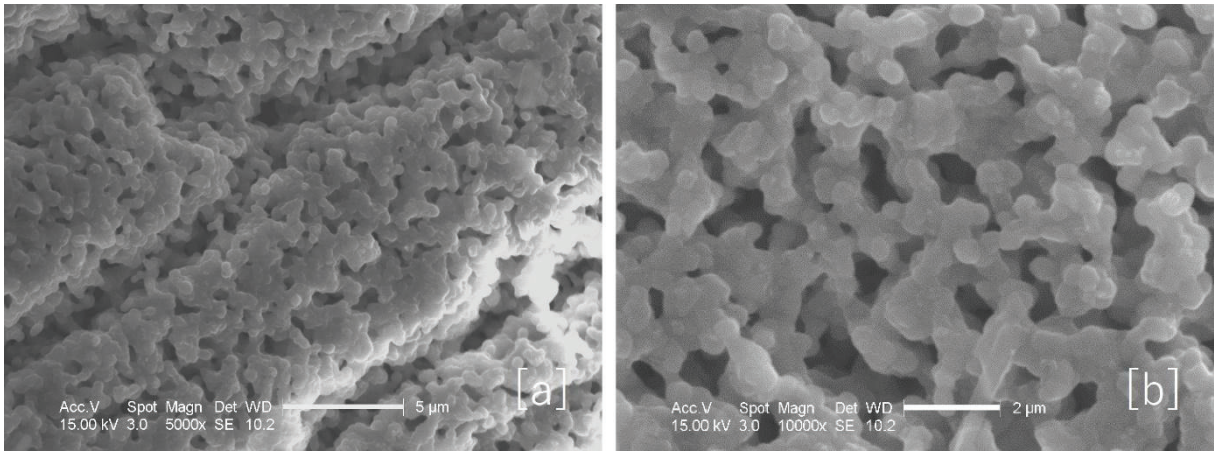

Fig. 7 – *Surface of the SO grain after thermal activation at 523 K, BSE, magnification: a) 5000x, b) 10000x*

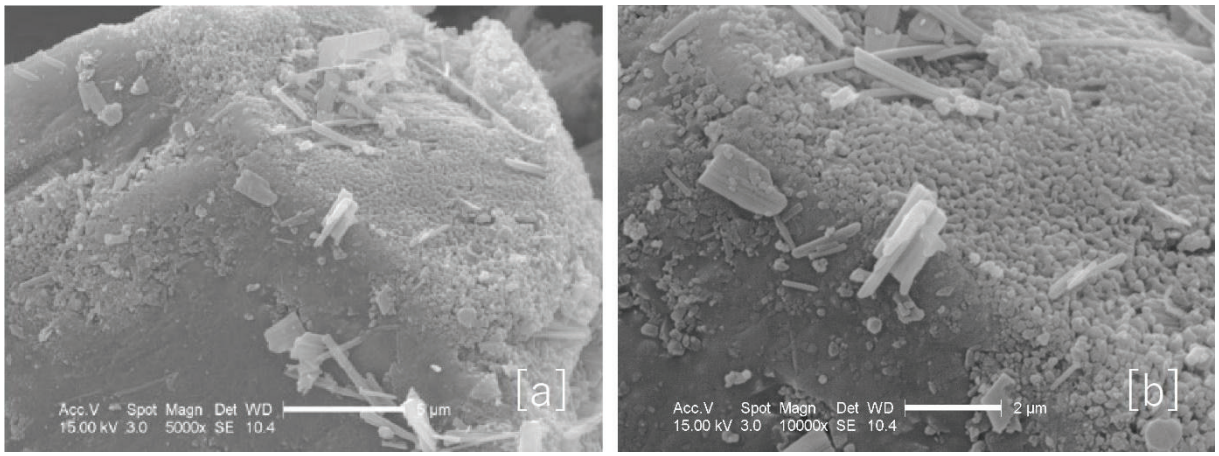

Fig. 8 – *Surface of the SOm grain after thermal activation at 373 K, BSE, magnification a) 5000x, b) 10000x*

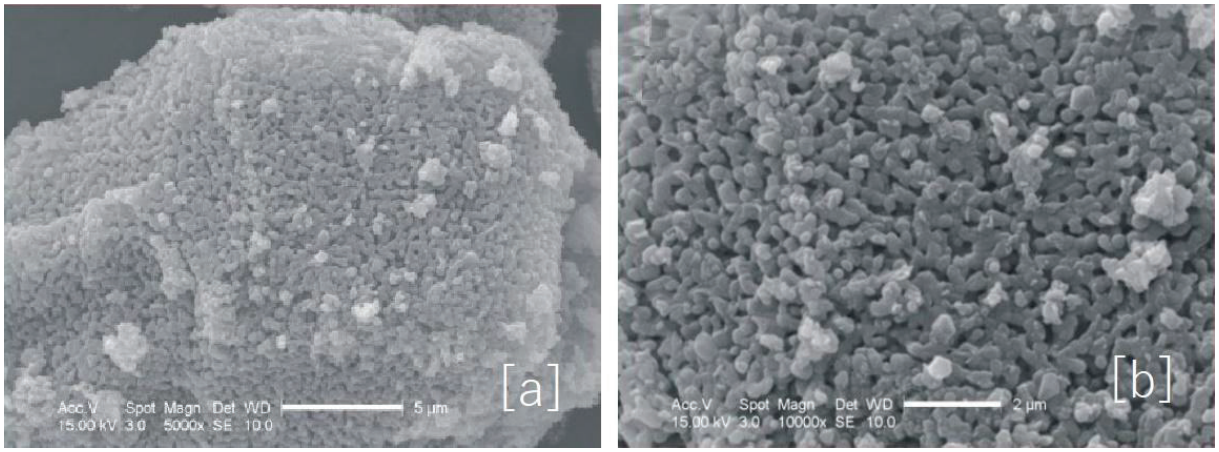

Fig. 9 – *Surface of the SOm grain after thermal activation at 523 K, magnification a) 5000x, b) 10000x*

Modification of ground $NaHCO_3$ (SOm) at 373 K resulted in developing numerous small pores which only partially covered the surface (Fig. 8). As the thermogravimetric analysis and the other tests showed[30], the decomposition of the ground sodium bicarbonate was not total, hence, the porous structure did not develop on the whole surface of the grains. Also, numerous lamellar and columnar crystals appeared of the size of several micrometers. After activation at 523 K, the crystals disappeared and the pores became more prominent, creating a well-developed, thick, porous layer (Fig. 9).

To determine the correlations of the characteristics of the surface area and the activation temperature, correlation coefficients were calculated, presented in Table 3. The calculations included SO and SOm thermally activated in the temperature range of 373–673 K. In such a temperature range, $NaHCO_3$ decomposed into Na_2CO_3. In both cases, the significance of the correlation was met ($r > 0$), which showed a strong correlation ($0.7 < r_{xy} < 0.9$).

The studies on circulating fluidized bed combustion rig verified the effect of grinding and heating of sodium reagents on their structural parame-

Table 3 – *Correlation coefficients of the specific surface area and the activation temperatures in the sodium compounds SO and SOm*

Tested characteristics	Sample	Correlation coefficient r_{xy}	Coefficient of determination R^2	Coefficient t_{kr}	Coefficient t	Fulfillment of the condition correlation $\lvert t \rvert > t_{kr}$
Surface area (LPNA) / activation temperature	SO	0.77	0.59	2.78	2.96	yes
	SOm	0.80	0.62		3.14	yes

ters. Their reactivity was determined in relation to sulphur dioxide and hydrogen chloride contained in the flue gases from combustion.

During combustion of coal only, the average emission of SO_2 at the outlet of the combustion chamber was 2829 mg m^{-3} and 24 mg m^{-3} of hydrogen chloride. After the samples were placed in the installation, a sudden drop in the pollutants followed. The SO and SOm sorbents were fed into the installation in three molar concentrations: 2Na/S: 0.5; 1.0 i 2.1. The use of SO sorbent resulted in the drop in the mean SO_2 concentration to the level of 2690–1830 mg m^{-3}.

The use of SOm sorbent decreased the mean SO_2 concentration to the level of 1660–490 mg m^{-3}. The achieved reduction levels of SO_2 are presented in Figs. 10 and 11. After the application of SO sorbent, the concentration of hydrogen chloride decreased from 24 mg m^{-3} to 6–7 mg m^{-3} and after the application of SOm sorbent it decreased to the level of 10–11 mg m^{-3}. Due to the significant excess of the sorbent in relation to the concentration of HCl in the gases, the change of the molar ration 2Na/S and not Na/Cl was taken into account. The effects of the application of SO and SOm in various molar ratios 2Na/S are presented in Figs. 12 and 13.

Each time after the introduction of sodium compounds into the flue duct, samples of fly ash (FA) were taken. In all the tested ash samples, chemical analyses confirmed presence of the products of the reaction in the form of sodium(IV, IV), sulphates, and sodium chlorides. The level of sodium(IV) sulphates were in the range of 0.03–0.2 %. The level of sodium(VI) sulphates in FA rose along with the increase in the molar ratio of 2Na/S and the decrease in the grain size from 4.6 % (for SO 2Na/S = 0.5) to 21.3 % (for SOm 2Na/S = 2.1).

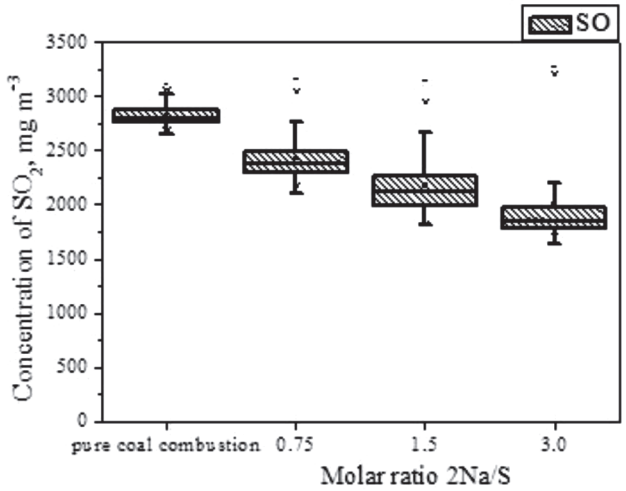

Fig. 10 – *Boxplot chart for the distribution of SO_2 concentration after using SO in different molar ratios*

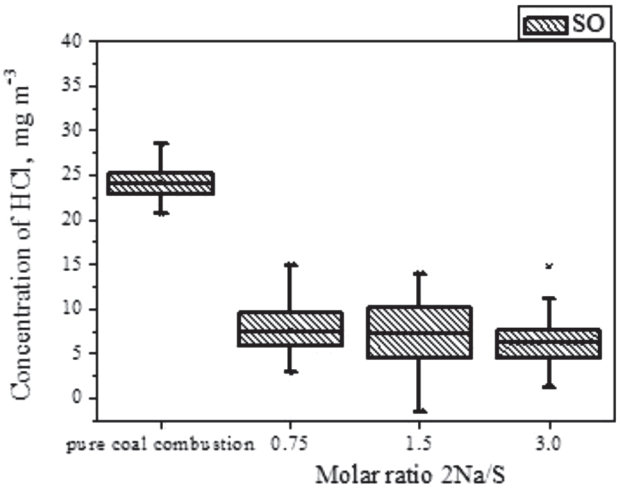

Fig. 12 – *Boxplot chart for the distribution of HCl concentration after using SO in different molar ratios*

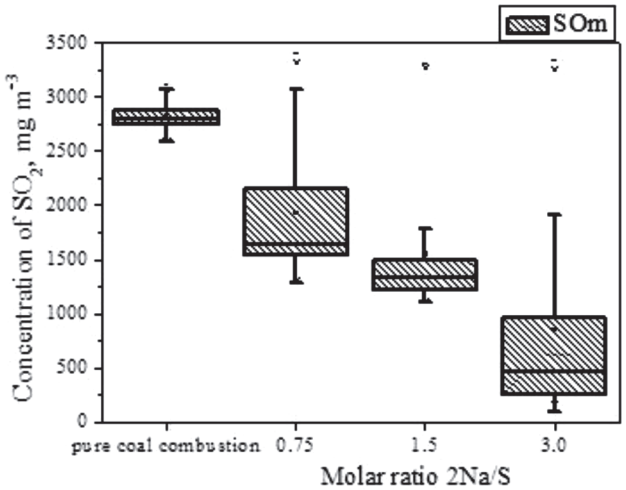

Fig. 11 – *Boxplot chart for the distribution of SO_2 concentration after using SOm in different molar ratios*

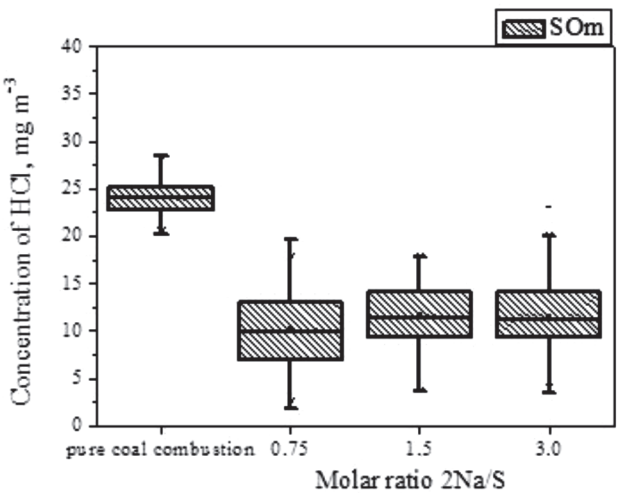

Fig. 13 – *Boxplot chart for the distribution of HCl concentration after using SOm in different molar ratios*

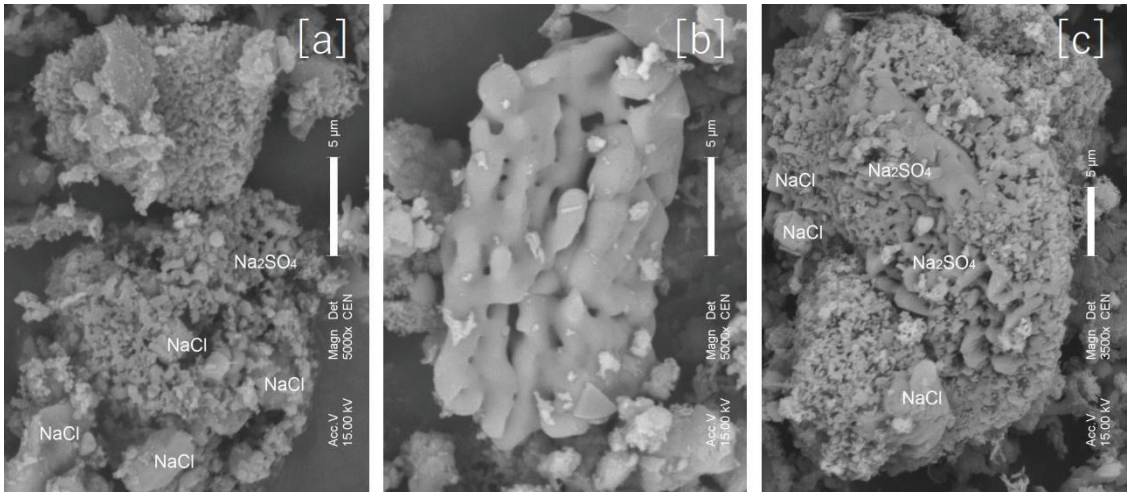

Fig. 14 – *Surface of the sodium compound, magnification: 5000x: a) Na_2CO_3 grain with embedded small particles of Na_2SO_4 and NaCl, b) sodium sulphate grain, c) expanded particles of Na_2SO_4 and NaCl embedded in Na_2CO_3*

In all the ash samples, presence of the product of the reaction of $NaHCO_3$ with hydrogen chloride in the form of sodium chloride was determined.

The following SEM images show the grains of sodium carbonate and embedded in them are smaller particles of sodium(VI) sulphate, calcium, crumbs of aluminosilicate enamel and efflorescence of sodium chloride forming several-micrometer-sized crystals.

Fig. 14a shows small particles of sulphate and sodium chloride of a size below a micrometer forming on a sodium carbonate grain. Some of the sodium sulphate grains combined (Fig. 14b) creating complex structures embedded in sodium carbonate grains (Fig. 14c).

Discussion

When removing SO_2 from flue gases, it was clearly observed that the grain size and the amount of the sorbent (molar ratio 2Na/S) affected the sorption effect. The small-grained SOm sorbent removed SO_2 better than SO sorbent. As the molar ratio increased, so did the efficiency of purification. The biggest drop in the SO_2 concentration was achieved at the molar ratio 2Na/S = 2.1 and the smallest at 2Na/S = 0.5.

When removing HCl, no clear influence of the grain size and the amount of the sorbent on the purification efficiency was observed. The application of SO sorbent with larger grains resulted in a greater drop in the HCl concentration than the application of SOm. Increasing the amount of the reagent only slightly improved the efficiency of removing HCl in SO sorbent, whereas in the case of SOm sorbent, it had no effect. Table 4 presents the achieved average and the minimum momentary concentrations of pollutants after placing the sorbents in the gas pipe.

The SO sorbent showed the smallest average SO_2 removal efficiency (equal to 17 %) at the smallest molar ratio (2Na/S = 0.5). At the 2Na/S = 2.1 ratio the efficiency was 35 %. The sorbent after

Table 4 – *Values of the average and the minimum concentration of SO_2 and HCl in the flue gas after the application of sodium compounds*

Type of sorbent	Molar ratio 2Na/S	Average concentration of SO_2	Minimum concentration of SO_2	Average concentration of HCl	Minimum concentration of HCl
Unit		mg m^{-3}	mg m^{-3}	mg m^{-3}	mg m^{-3}
SO	0.5	2353	2112	8.4	2.9
	1.0	2074	1806	7.8	4.1
	2.1	1839	1632	5.3	1.2
SOm	0.5	1582	1282	10.4	1.8
	1.0	1294	1104	10.9	5.0
	2.1	317	98	11.2	3.4

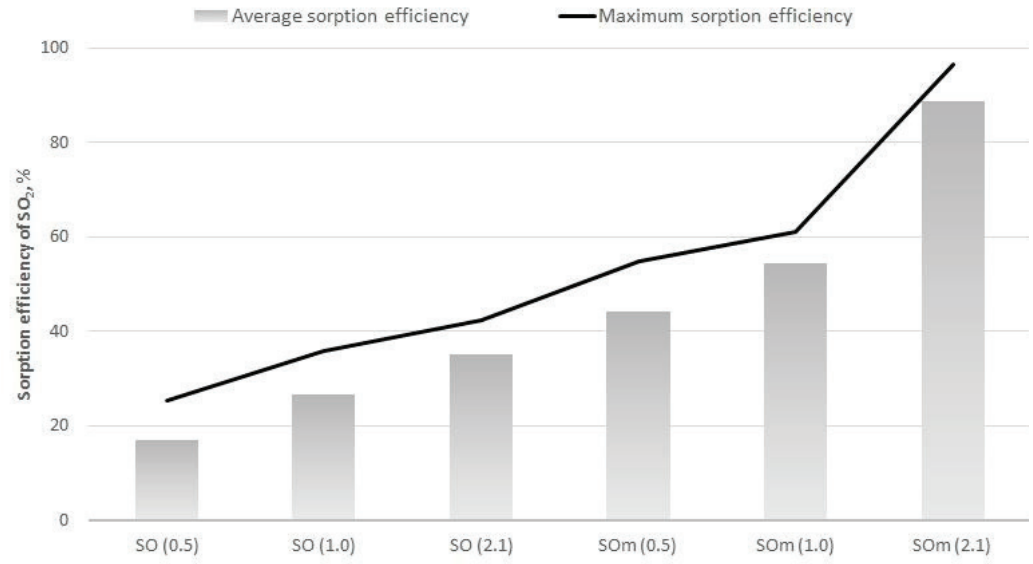

Fig. 15 – *Average and maximum sorption efficiency of SO_2 after the application of sodium compounds in various molar ratios*

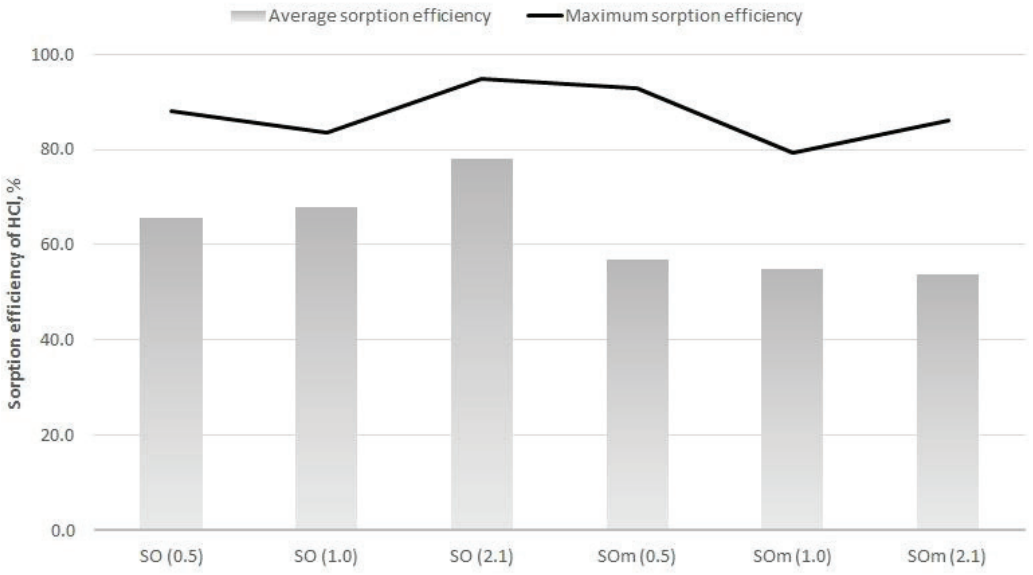

Fig. 16 – *Average and maximum sorption efficiency of HCl after the application of sodium compounds in various molar ratios*

grinding – SOm had the average sorption efficiency twice as great as that of SO at the molar ratio of 2Na/S = 2.1.

Increasing the amount of the reagent improved the purification efficiency up to as much as 89 % for 2Na/S = 2.1. The maximum momentary purification efficiency by SO sorbent was 25–42 %, and by SOm from 55 % to 97 %. The values of the average and the maximum SO_2 removal efficiency is presented in Fig. 15.

The average HCl removal efficiency was above 50 %. When using the SO reagents, the average efficiency was from 66 % to 78 %, and when using SOm it was in the range of 54–57 %. The maximum efficiency was at the level of 79–95 %. The values of the average and the maximum HCl removal efficiencies are presented in Fig. 16.

Summary

The laboratory studies and the studies on the circulating fluidized bed combustion rig CFB showed that properly prepared sodium sorbents work very well in the dry method of purification of fumes from the combustion of coal.

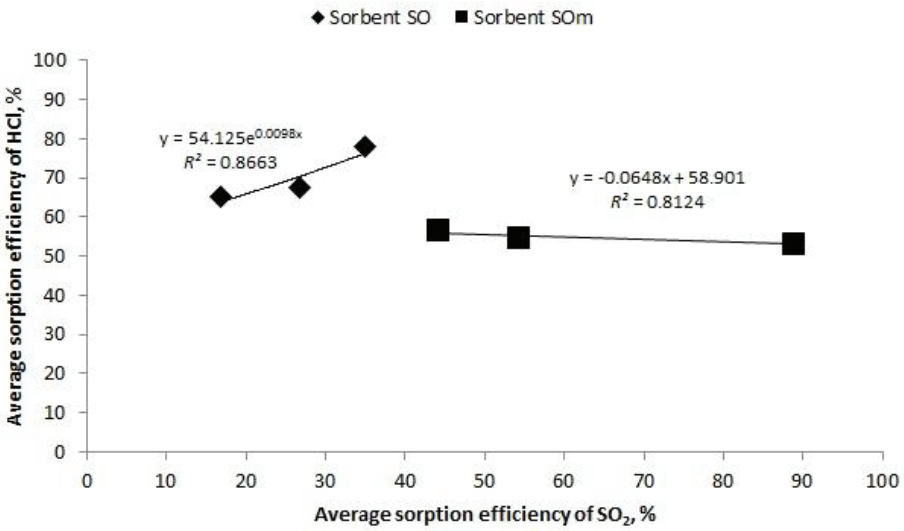

Fig. 17 – *Correlation of the average sorption efficiency of SO_2 and HCl after the introduction of sorbents*

Grinding and heating resulted in the change of the surface topography of the grains of the sodium sorbents. The unground grains (SO) had smooth surface without pores and after grinding they changed into forms that had furrows and cracks. After heating in the temperature range of 373–673 K, the grains intensively developed their surface area. Their pore structure was thick and extensive, and it covered almost the whole surface of the grains.

After grinding, the microstructure (LPNA) of the surface area did not change significantly – from 0.09 $m^2\ g^{-1}$ do 0.73 $m^2\ g^{-1}$. The macrostructure (MIP) of the surface area increased from 0.13 $m^2\ g^{-1}$ do 1.02 $m^2\ g^{-1}$, and the pore volume from 0.06 $cm^3\ g^{-1}$ do 0.36 $cm^3\ g^{-1}$. After heating, the surface area (LPNA) of SO was about 3 $m^2\ g^{-1}$, and SOm up to approximately 6 $m^2\ g^{-1}$.

The increase in the surface area (LPNA) of the ground sorbent SOm was much higher than in the unground sorbent SO. After heating, the surface of the SO (MIP) was over 4 $m^2\ g^{-1}$ and the pore volume up to 0.77 $cm^3\ g^{-1}$.

Grinding also resulted in the decrease in the decomposition temperature of the sodium bicarbonate. The maximum decomposition of the SO sample occurred at 431 K, whereas the decomposition of SOm occurred at 414 K. Grinding also improved the purification speed from acid gas components. The accessibility of the surface of the sorbent grains improved, and thus the purification process could proceed faster.

When removing SO_2 from flue gases, it was observed that the grain size and the amount of the sorbent (molar ratio 2Na/S) affected the sorption efficiency. The average SO_2 removal efficiency of SOm was several times as high as before grinding (SO). The highest average sorption efficiency in the case of both reagents was achieved at the largest molar ratio 2Na/S = 2.1. In the case of SO it was 35 %, and in the case of SOm 89 %.

The process of hydrogen chloride removal from sulphurised flue gas that took place simultaneously was highly efficient. Regardless of the grinding degree and the molar ratio 2Na/S, the average HCl removal efficiency was from 54 % to 78 %. The correlation of the average sorption efficiencies of SO_2 and HCl are presented in Fig. 17.

After sorption on the surface, used sorbents, the products of sorption of SO_2 (sodium(IV, VI) sulphate) as well as product of sorption of hydrogen chloride (NaCl), stay mainly on the surface of the sample grains. Sulphur dioxide, which is present in flue gases in higher concentrations than hydrogen chloride, does not inhibit the absorption of that pollutant.

The results of the analyses prove that properly prepared sodium compounds have the ability to almost completely simultaneously remove SO_2 and HCl from purified flue gases. They can therefore be successfully used in conventional power industry.

ACKNOWLEDGMENTS

This work was funded by the National Centre for Research and Development as part of the project called 'Modified sodium bicarbonate in dry purification of flue gases in various industrial facilities' (Project No. NR05000910), and by the European Social Fund as part of the project called 'Scientific scholarships as a chance for the development of The Voivodeship of Silesia' (Project No. POKL.08.02.01-24-019/11).

References

1. *Pajdak, A., Zarębska, K., Walawska, B., Szymanek, A.,* Removing SO_2 from solid fuel combustion gases by the use of sodium sorbents, Przem. Chem. **94/3** (2015) 382. doi: https://doi.org/10.15199/62.2015.3.25
2. *Pilat, M. J., Wilder, J. M.,* Pilot scale SO_2 control by dry sodium bicarbonate injection and an electrostatic precipitator, Environ. Prog. Sustain. Energy **26** (3) (2007) 263. doi: https://doi.org/10.1002/ep.10212
3. *Raclavska, H., Matysek, D., Raclavsky, K., Juchelkova, D.,* Geochemistry of fly ash from desulphurisation process performed by sodium bicarbonate, Fuel Process. Technol. **91** (2010) 150. doi: https://doi.org/10.1016/j.fuproc.2009.09.004
4. *Kong, Y., Wood, M. D.,* Dry injection of sodium sorbents for air pollution control, Period Am. Acad. Environ. Eng. **47** (2011) 20.
5. *Kolat, P., Čech, B., Vrtek, M., Tomášek, D.,* Experiments on additive desulphurisation by sodium bicarbonate in coal-fuel boilers, Chem. Process Eng. **34** (1) (2013) 77. doi: https://doi.org/10.2478/cpe-2013-0007
6. *Święszek, G.,* The use of sodium bicarbonate to neutralize acid compounds in flue gases, Instal. **7/8** (2014) 23.
7. *Keener, T. C., Khang, S.,* Kinetics of the sodium bicarbonate – sulfur dioxide reaction, Chem. Eng. Sci. **48** (16) (1993) 2859.
8. *Garding, M., Svedberg, G.,* Modelling of dry injection flue gas desulfurization, JAPCA. **38** (10) (1988) 1275. doi: https://doi.org/10.1080/08940630.1988.10466974
9. *Kimura, S., Smith, J. M.,* Kinetics of the sodium carbonate – sulfur dioxide reaction, AIChE Journal. **33** (9) (1987) 1522. doi: https://doi.org/10.1002/aic.690330912
10. *Wu, C., Khang, S. J., Keener, T. C., Lee, S. K.,* A model for dry sodium bicarbonate duct injection flue gas desulfurization, Adv. Environ. Res. **8** (3–4) (2004) 655. doi: https://doi.org/10.1016/S1093-0191(03)00038-8
11. *Fellows, K. T., Pilat, M. J.,* HCl sorption by dry $NaHCO_3$ for incinerator emissions control, J. Air Waste Management Assoc. **40** (6) (1990) 887.
12. *Kong, Y., Davidson, H.,* Dry Sorbent Injection of Sodium Sorbents for SO_2, HCl and Mercury Mitigation, 18th Annual North American Waste-to-Energy Conf., 2010, Orlando, Florida, USA
13. *Wielgosiński, G., Zawadzka, A.,* Analiza skuteczności różnych reagentów w procesie usuwania HCl ze spalin w spalarni odpadów medycznych metodą suchą, POL-EMIS 2012 Conf. Wroclaw, Poland 2012, 319.
14. *Pająk, T.,* Zagospodarowanie osadów ściekowych metodami termicznymi, monograph, University of Technology and Humanities Publ., Radom 2013.
15. *Haramija, V.,* Carbon capture and storage technologies, GOMABN. **51** (4) (2012) 306.
16. *Baran, P., Zarębska, K., Czuma, N.,* CO_2 adsorption properties of char produced from brown coal impregnated with alcohol amine solutions, Environ. Monit. Assess. **188** (2016) 416. doi: https://doi.org/10.1007/s10661-016-5423-z
17. *Dindi, A., Quang, D. V., Abu-Zahra, M. R. M.,* Simultaneous carbon dioxide capture and utilization using thermal desalination reject brine, Applied Energy **154** (2015) 298. doi: https://doi.org/10.1016/j.apenergy.2015.05.010
18. Directive 2001/80/EC of the European Parliament and of the Council of 23 October 2001 on the limitation of emissions of certain pollutants into the air from large combustion plants, Official Journal of the European Union L 309.
19. Directive 2010/75/EU of the European Parliament and of the Council of 24 November 2010 on industrial emissions (integrated pollution prevention and control), Official Journal of the European Union L334/17.
20. Directive 2015/2193 of the European Parliament and of the Council of 25 November 2015 on the limitation of emissions of certain pollutants into the air from medium combustion plants.
21. Directive 2000/76/EC of the European Parliament and of the Council of 4 December 2000 on the incineration of waste. Official Journal of the European Union L 332.
22. Reference Document on BAT for Large Combustion Plants. TL/JFF/FN/EIPPCB/LCP_Final Draft (2016), http://eippcb.jrc.ec.europa.eu (05.2016)
23. Solvay brochure, 2014, www.solvairsolutions.com (02.2015)
24. *Jain, R. C.,* Manufacture of soda ash by modified Solvay process, Chem. Eng. World **19** (4) (1982) 65.
25. *Brunauer, S.,* Physical Adsorption. Princeton University Press, Princeton, 1945.
26. *Rouquerol, J., Baron, G., Denoyel, R., Giesche, H., Groen, J., Klobes, P., Levitz, P., Neimark, A. V., Rigby, S., Skudas, R., Sing, K., Thommes, M., Unger, K.,* Liquid intrusion and alternative methods for the characterization of macroporous materials (IUPAC Technical Report), Pure Appl. Chem. **84** (1) (2012) 107. doi: https://doi.org/10.1351/PAC-REP-10-11-19
27. *Czakiert, T., Sztekler, K., Karski, S., Markiewicz, D., Nowak, W.,* Oxy–fuel circulating fluidized bed combustion in a small pilot-scale test rig, Fuel Process. Technol. **91** (2010) 1617. doi: https://doi.org/10.1016/j.egypro.2014.11.039
28. US4588569. Dry injection flue gas desulfurization process using absorptive soda ash sorbent (1986).
29. *Rouquérol, J., Avnir, D., Fairbridge, C. W., Everett, D. H., Haynes, J. H., Pernicone, N., Ramsay, J. D. F., Sing, K. S. W., Unger, K. K.,* Recommendations for the characterization of porous solids (Technical Report) Pure and Applied Chemistry **66** (8) (1994)1739. doi: https://doi.org/10.1351/pac199466081739
30. *Walawska, B., Szymanek, A., Pajdak, A., Szymanek, P.,* Impact of temperature distribution on the surface area of sodium bicarbonate, Przem. Chem. **91** (5) (2012) 1049.